ACS SyntheticBiology

pubs.acs.org/synthbio

Research Article

Optogenetic Modification of *Pseudomonas aeruginosa* Enables Controllable Twitching Motility and Host Infection

Aiguo Xia, Mingjie Qian, Congcong Wang, Yajia Huang, Zhi Liu,* Lei Ni,* and Fan Jin*

Cite This: *ACS Synth. Biol.* 2021, 10, 531−541

Read Online

ACCESS | Metrics & More | Article Recommendations | Supporting Information

ABSTRACT: Cyclic adenosine monophosphate (cAMP) is an important secondary messenger that controls carbon metabolism, type IVa pili biogenesis, and virulence in *Pseudomonas aeruginosa*. Precise manipulation of bacterial intracellular cAMP levels may enable tunable control of twitching motility or virulence, and optogenetic tools are attractive because they afford excellent spatiotemporal resolution and are easy to operate. Here, we developed an engineered *P. aeruginosa* strain (termed *pactm*) with light-dependent intracellular cAMP levels through introducing a photoactivated adenylate cyclase gene (*bPAC*) into bacteria. On blue light illumination, *pactm* displayed a 15-fold increase in the expression of the cAMP responsive promoter and an 8-fold increase in its twitching activity. The skin lesion area of nude mouse in a subcutaneous infection model after 2-day *pactm* inoculation was increased 14-fold by blue light, making *pactm* suitable for applications in controllable bacterial host infection. In addition, we achieved directional twitching motility of *pactm* colonies through localized light illumination, which will facilitate the studies of contact-dependent interactions between microbial species.

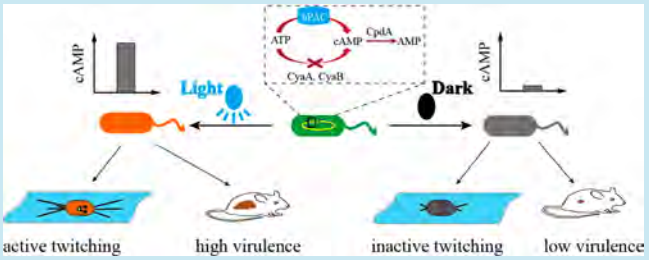

KEYWORDS: *optogenetic manipulation, cyclic adenosine monophosphate, Pseudomonas aeruginosa, host infection*

Cyclic adenosine monophosphate (cAMP) is a ubiquitous second messenger involved in cell signaling in response to various environmental factors.[1−3] cAMP is usually synthesized from adenosine triphosphate (ATP) molecules by adenylate cyclases, and development of light-responsive adenylate cyclase (LRAC) offers the means to control intracellular cAMP level using light.[4−8] With LRAC, researchers can easily generate transient or local pulses of cAMP concentration in cells, which was extensively used to study neuronal signaling, fertilization, and subcellular signal transduction in mammalian cells.[9−14] By far, there are relatively few applications of LRAC in bacteria. In fact, cAMP regulates multiple important cellular processes in a variety of bacterial species, including the regulation of carbon metabolism, motility, cytotoxicity and virulence.[15−20] Therefore, manipulating the intracellular cAMP level in these bacteria using LRAC may afford optical control of many bacterial phenotypes.

Pseudomonas aeruginosa is one of the most representative organisms where the physiological role of cAMP was extensively studied. The virulence factor Vfr acts as the main effector of cAMP in *P. aeruginosa*, and high levels of cAMP greatly increase the transcription of numerous genes, such as type II and III secretion systems and type IVa pili (TFP).[15,21−26] The cAMP-Vfr complex controls TFP biogenesis by collectively regulating multiple TFP components including the motor ATPases PilBTU, the alignment subcomplex PilMNOP, the secretin PilQ, and the PilSR two-component system that regulates PilA levels.[26] Therefore, manipulation of intracellular cAMP level is sufficient to control bacterial twitching activity, which is difficult to achieve by adjusting the expression of one or two TFP structure genes. TFP-mediated twitching motility is a key action for *P. aeruginosa* to break through the ciliated airway epithelium of the host.[27] Similarly, cAMP-Vfr also control the expression of the type III secretion system genes through the master regulator ExsA,[24] control the expression of the exotoxin ToxA directly through transcription and indirectly through transcriptional factors ToxR and PtxR.[28−30] Thus, virulence of *P. aeruginosa*, especially acute virulence, is sensitive to the bacterial cellular cAMP content. Here, taking *P. aeruginosa* as chassis, we aimed for an optogenetic tool that allows precise control of intracellular cAMP concentration, thereby enabling the manipulation of twitching motility and bacterial virulence using light. We developed an engineered *P. aeruginosa* strain (*pactm*) based on a photoactivated adenylate cyclase reported previously.[7] Twitching activity of the strain is sensitive to weak light and changes reversibly under light-dark switch. In addition, host infection of *pactm* increased 14-fold upon light

Received: November 5, 2020
Published: March 5, 2021

https://dx.doi.org/10.1021/acssynbio.0c00559
ACS Synth. Biol. 2021, 10, 531−541

illumination after 2-day subcutaneous inoculation in mouse, making *pactm* a suitable tool for the study of host−pathogen interactions.

RESULTS

Design of an Engineered Strain to Manipulate Intracellular cAMP Level *via* Optogenetic Tool. In our two-step strategy (Figure 1A), we first incorporated an optogenetic module into the chromosome of *P. aeruginosa* using the mini-CTX system.[31] The photoactivated adenylate cyclase (bPAC) can cyclize adenosine triphosphate (ATP) to form cAMP in the presence of blue light.[7] *pabPAC* is the codon-optimized version of the original *bPAC* for proper expression in *P. aeruginosa*. We used a constitutive promoter (*J23100*) to control the transcription of *pabPAC*. Second, we knocked out both *cyaA* and *cyaB* from the chromosome to reduce the background level of cAMP. In wild type *P. aeruginosa*, CyaA and CyaB are the two adenylate cyclases for cAMP synthesis, and CpdA is the only phosphodiesterase for cAMP degradation.[21,22,26] Under blue light illumination, the combined action of bPAC and CpdA should lead the intracellular cAMP concentration to an equilibrium value. While after removing of blue light, CpdA would constitutively degrade cAMP to background level. Therefore, this optogenetic system enables the precise manipulation of cAMP concentration in *P. aeruginosa*, thereby enabling the manipulation of bacterial twitching activity and virulence using blue light. The resultant strain was termed *pactm* (*P. aeruginosa* with controllable twitching motility). To monitor the intracellular cAMP levels, we introduced a plasmid encoding a green fluorescent protein (SfGFP) driven by a cAMP regulatory promoter (*Plac*) and an orange fluorescent protein (CyOFP1) downstream of a constitutive promoter (*J23102*) (Figure 1A). We analyzed SfGFP intensity as a read-out for intracellular cAMP levels, and the CyOFP1 expression is for unified cell recognition during image processing. The response of intracellular cAMP level in *pactm* upon blue light illumination was confirmed using ELISA method (Figure 1B), cAMP concentration in *pactm* exhibited a 6.6-fold increase by blue light. And as expected, cAMP level of PAO1 wild type cells did not exhibit significant difference upon blue light illumination. In addition, cAMP level in *cpdA* mutant cells is much higher than that in *pactm* and wild type cells, indicating the key role of CpdA in cAMP degradation.

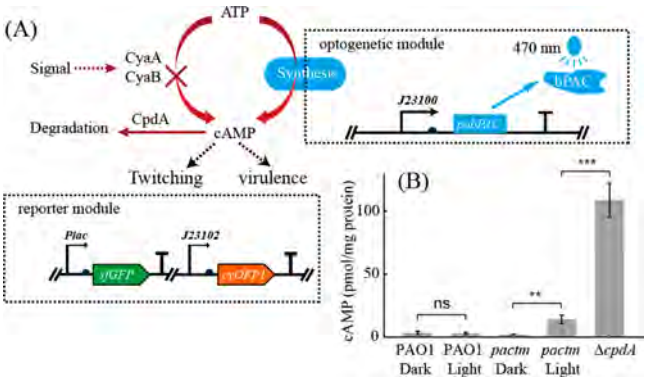

Figure 1. (A) Schematic representation of the optogenetic, reporter modules and gene modifications in the engineered *pactm* strain. The adenylate cyclase-encoding genes *cyaA* and *cyaB* were deleted from the chromosome of *P. aeruginosa* to eliminate background cAMP level. Codon-optimized bPAC (*pabPAC*), together with the constitutive J23100 promoter, were inserted into the chromosomal CTX site. A two-color reporter plasmid was introduced later to monitor the intracellular cAMP level. (B) Intracellular cAMP levels of PAO1 wild type, *pactm* or *cpdA* mutant cells under blue light illumination or darkness. cAMP concentrations were determined by ELISA method. Blue light intensity was 750 μW/cm^2 in all light group experiments.

Response of Intracellular cAMP Level and Twitching Motility upon Blue Light Illumination in *pactm*. We measured the intracellular cAMP levels and speed of twitching motility of *pactm* cells under light illumination and darkness. Experiments were conducted in flow chambers to enable cell growth under constant nutrient supplementation. We used automated cell tracking to follow surface-attached cells, and to record SfGFP intensity of each cell. Our method allows us to follow large numbers of attached cells and quantify their twitching activity and cAMP levels simultaneously. Under blue light illumination, *Plac* expression was increased 15-fold compared to the levels of expression in cells under darkness (Figure 2A, 2B, and 2E), indicating an increased cAMP level in *pactm*. Meanwhile, twitching motility of cells under light illumination is strongly biased toward high speed, the mean speed of cells was 0.16 μm/s (Figure 2D, 2E, and Movie S1), which is 8-fold the cell speed under darkness (0.02 μm/s) (Figure 2C, 2E, and Movie S2). These data demonstrate that twitching motility in *pactm* is capable of responding to blue light.

We further examined how the dose of blue light illumination influence cAMP level and cell speed. *Plac* expression exhibited a sigmoidal curve in response to increasing blue light intensity (Figure 2F). *Plac* expression was detectable at light irradiation larger than 5 μW/cm^2, increased linearly with the logarithm of light intensity, and reached saturation at 400 μW/cm^2 (Figure 2F). Similarly, cell speed in response to increasing light intensity also exhibited a sigmoidal shape and saturated at 400 μW/cm^2, but was more sensitive to weak illumination; cell speed under 5 μW/cm^2 illumination was twice as high as that in dark condition (Figure 2G). Therefore, twitching motility in the *pactm* strain was sensitive to blue light.

Characterization of Light-Induced Twitching Motility in *pactm*. We further analyzed the trajectories of *pactm* cells under light illumination from bright-field microscopy movies by using a simplified version of our previously reported twitching analysis method.[32] Two parameters, k_{MSD} and θ, were used to divide twitching motility into three types, *i.e.*, walking ($\theta > 0$), wiggling ($\theta = 0$, $k_{MSD} < 1.5$), and crawling ($\theta = 0$, $k_{MSD} > 1.5$). θ is the time-averaged tilt angle of the bacterial long axis with respect to surface. $\theta = 0$ corresponds to two poles attached to surface, and $\theta > 0$ corresponds to one pole attached to surface. k_{MSD} is the slope of mean-squared displacement curve of bacterial trajectory. $k_{MSD} = 1.0$ corresponds to random diffusive motion, whereas $k_{MSD} = 2.0$ corresponds to directional ballistic motion. The walking cells attach to the surface with one pole and alter their twitching directions frequently, resulting in a high angular speed. Wiggling cells are bipolar attached and usually generate low net translational motion. Crawling cells are also bipolar attached and tend to generate high net translational motion. Both wiggling and crawling cells have low angular speed.

In comparison to twitching motility of cells in darkness, *pactm* under blue light illumination exhibit significant less wiggling type cells (light 6%, dark 36%, $P < 0.01$), nearly equal

https://dx.doi.org/10.1021/acssynbio.0c00559
ACS Synth. Biol. 2021, 10, 531−541

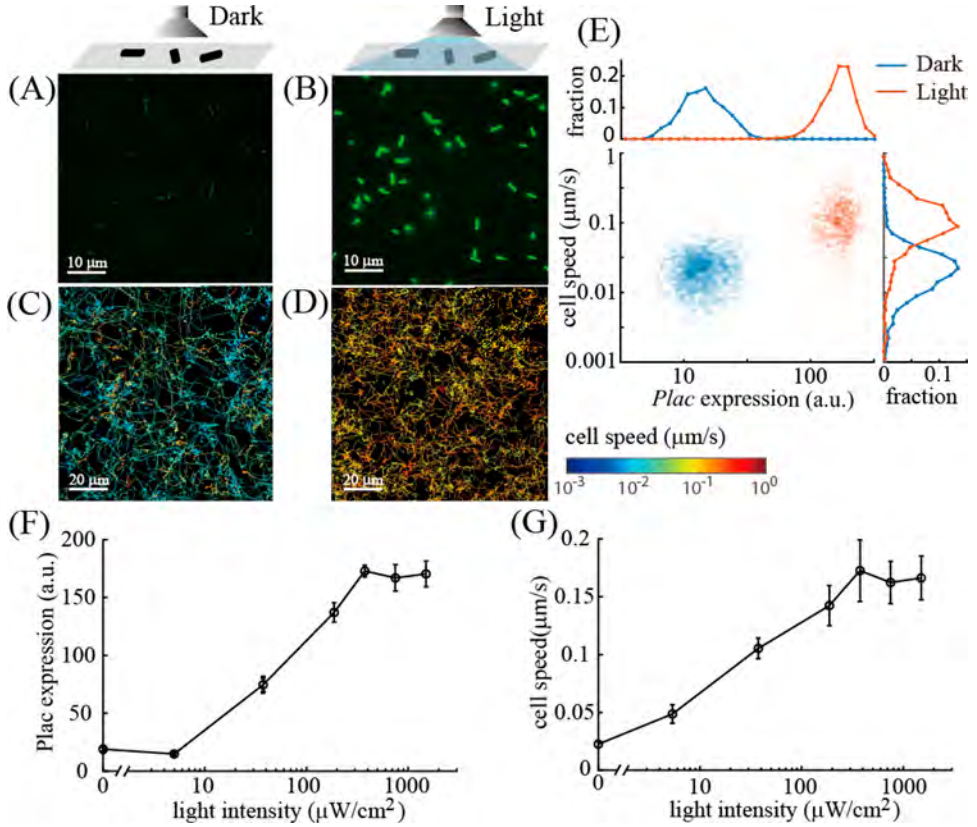

Figure 2. Response of *Plac* expression and twitching motility of *pactm* to blue light. (A,B) SfGFP fluorescent image of cAMP reporter in *pactm* under dark condition (A) or under 6-h blue light illumination. (C,D) Trajectories of the *pactm* cells in dark condition or under 6-h blue light illumination, the color on each trajectory indicates the corresponding time average of cell speed. (E) Cell speed plotted against *Plac* expression in *pactm* cells under darkness (blue dot) or blue light illumination (red dot) for 6 h, each data point in the map indicates the data from a single cell. The distribution curves of cell speed or *Plac* expression were shown on the side. (F,G), Mean value of *Plac* expression (F) or mean cell speed (G) as a function of blue light intensity illuminated on *pactm* cells. Data in F and G are shown as the mean ± s.d.

fraction of crawling type cells (light 45%, dark 48%, $P > 0.05$), and more walking type cells (light 49%, dark 16%, $P < 0.05$) (Figure 3A). Meanwhile, both cell speed and cell angular speed are increased in all three motility types in response to blue light illumination (Figure 3B, Figure 3C), indicating a complete activation of twitching motility in *pactm*. The angular speed distribution curve of light-irradiated cells displayed a bimodal pattern (Figure 3D), indicating a sharp gap in angular speed between crawling and walking. Moreover, the distribution of k_{MSD} was biased toward 2.0 under light illumination (Figure 3D), suggesting that light-exposed cells favor ballistic motion. In addition, compared to the cells kept in darkness, blue light-illuminated cells move more toward the sides of bacterial axis, indicating the direction change of TFP extension (Figure 3E).

To investigate whether the upregulated twitching activity was due to the general effect of blue light on bacteria, we compared the twitching motility under light illumination and darkness of PAO1 wild type cells. As shown in Figure S2, PAO1 wild type cells exhibited similar profile for the fraction of different motility types under light illumination and darkness. However, cell speeds of walk-type and crawling-type cells under darkness were about twice of that under light illumination, and the angular speed of walk-type cells also exhibited 50% reduction upon light illumination. Therefore, blue light has a slightly negative effect on the twitching motility of wild type *P. aeruginosa*. In addition, blue light also exhibited slight inhibition on twitching activity of *pactm* Δ*vfr* cells (Figure S3), confirming that Vfr is central regulator that mediate the upregulated twitching motility of hyper-cAMP cells. Taken together, our results demonstrate that blue light comprehensively induced the twitching activity in *pactm* through the action on bPAC.

At present, we are unable to disclose the exact quantitative relationship between pili number and bacterial twitching phenotype. A hypothesis is summed below: Bacterial cell will be pulled by a single TFP only when the distal tip of the filament is adsorbed to the substratum and the filament is retracted by actuators simultaneously. According to one previous study, this pulling process constitutes only a small time fraction of the whole pilus movement cycle.[33] Therefore, we tend to believe that there is a relatively linear relationship between frequency of cell movement and TFP number when TFP number is not too large, which could explain the increased mean cell speed of crawling cells with high cAMP level. When blue light illumination is within the range of 5−375 $\mu W/cm^2$, both Plac expression and cell speed increased linearly with light intensity (Figure 2F, Figure 2G); this is consistent to our hypothesis. On the other hand, *P. aeruginosa* cells use TFP to walk upright, and cells without TFP cannot walk on surfaces.[34] Moreover, wiggling cells of *pactm* in dark condition are probably cells with very few TFP, according to their extremely low cell speed and angular speed (Figure 3B and Figure 3C). Therefore, *pactm* cells under light illumination (with more TFP) exhibit more walking cells and less wiggling cells.

https://dx.doi.org/10.1021/acssynbio.0c00559
ACS Synth. Biol. 2021, 10, 531−541

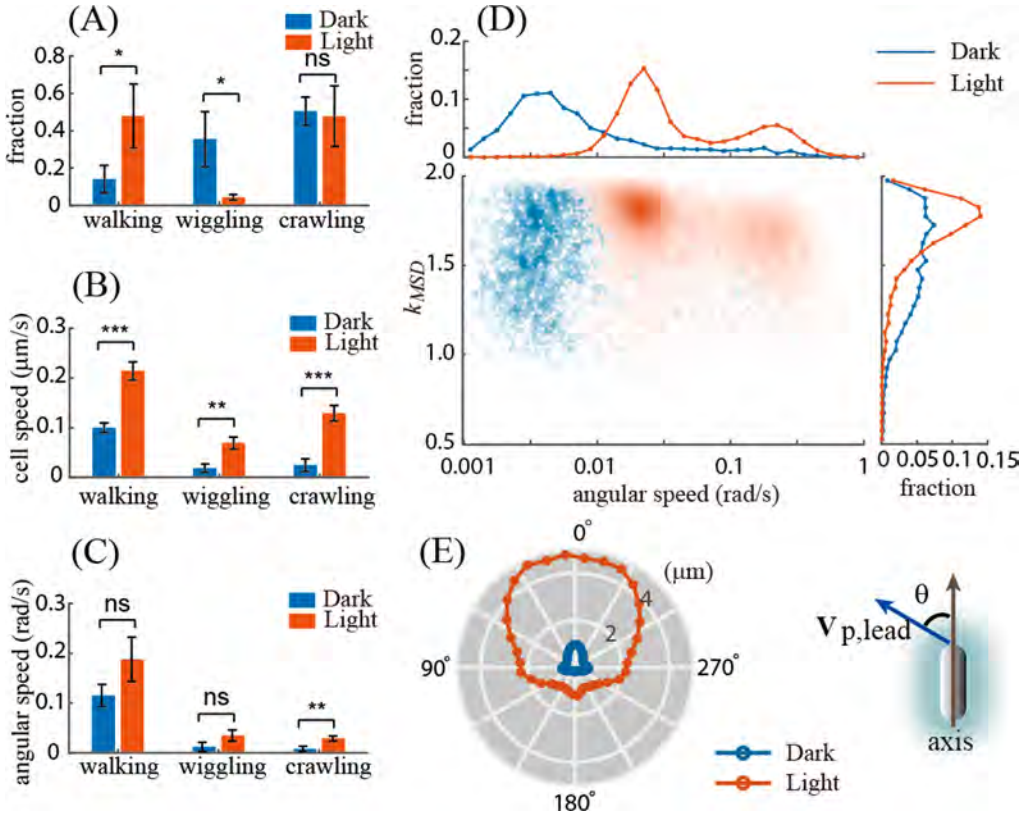

Figure 3. Detailed characterization of twitching motility of *pactm* cells with or without blue light illumination. (A,B,C) Fraction (A) or mean cell speed (B), or mean angular speed (C) of cells with different motility types under darkness (blue bar) or after 6-h blue light illumination (red bar). (D) Slope of the mean-squared displacement k_{MSD} as a function of angular speed of cells under darkness (blue dot) or after 6-h blue light illumination (red dot), each data point in the map indicate the data from a single cell, the distribution curves of k_{MSD} or cell angular speed were shown on the side. (E) Mean displacement at different deviation angles in 1000 s calculated from >1000 trajectories of different single *pactm* cells under darkness (blue) or after 6-h blue light illumination (red). Statistical analysis based on ANOVA method (ANOVA2 function in MATLAB). $^*P < 0.05$; $^{**}P < 0.01$; $^{***}P < 0.001$; ns, nonsignificant.

Dynamics and Reversibility of Twitching Manipulation in *pactm*. To test the reversibility of twitching manipulation in *pactm*, we switched the culture conditions between light illumination and darkness, and monitored *Plac* expression and mean cell speed over time. When we moved cells from dark to light, *Plac* expression increased instantly and homogeneously across the population (Figure 4A). Time dependent response of *Plac* expression followed an S-shaped curve with a halftime of approximately 3 h (Figure 4C). Meanwhile, mean speed of twitching motility also increased instantly upon blue light illumination, but entered a plateau earlier than *Plac* expression, with a halftime of only 2 h (Figure 4A, Figure 4D). Considering pili assembly is a relatively rapid process,[33,35] the long response time of *pactm* should be attributed to the lengthy processes of cAMP accumulation and protein expression. By contrast, when we moved cells from light to dark, both *Plac* expression and mean cell speed decreased near-exponentially with time, with a common 2-h half-decay time (Figure 4B, 4C, and 4D). Bacteria lose their TFP through the dilution effect of cell division, and the mean division time for cells in the experiment is 1.5 h. According to the fact that bPAC loses the adenylate cyclase activity rapidly (<20 s) following the removal of blue light,[7] the 0.5-h delay may come from the process of cAMP degradation by CpdA. To conclude, twitching motility in *pactm* could be reversibly manipulated using blue light and the characteristic response time is 2 h.

Optical Manipulation of Directional Propagation of Bacterial Colonies. Since elevated level of intracellular cAMP only upregulates the total expression of TFP, the light-bPAC-cAMP strategy presented here does not enable controlling of the direction of twitching motility at single cell level. However, at the macroscopic level, optical guidance of the propagation direction of bacterial population is possible. To set up an experimental system, we grew bacterial colonies under agarose plates using standard stab assay.[36] Our experiments for *pactm* cells failed to exhibit any increase of the colony expansion area (Figure S1), which is consistent with Fulcher's result that cAMP deplete/replete bacteria have minimal effects on their twitching zones.[22] We later found that the effect of cAMP on twitching zone was only apparent when the flagella were absent, although it is not clear whether there is a synergistic effect between the flagella and the pili. As a control experiment, blue light illumination did not affect the twitching zone of wild type Δ*fliC* cells (Figure S1).

The radius of twitching zone of the *pactm*Δ*fliC* strain under light illumination was 4-fold ($P < 0.001$) the radius under dark conditions (Figure 5A, Figure 5B), indicating that it is feasible to manipulate twitching motility of bacterial colonies under plate. Assuming the illumination of a specific colony-containing area, cells within this area move actively while slow down as they cross the edges of the illuminated area. The barrier formed by stacked cells near the edge would prevent the crossing of subsequent bacteria, thus the net result is that

https://dx.doi.org/10.1021/acssynbio.0c00559
ACS Synth. Biol. 2021, 10, 531−541

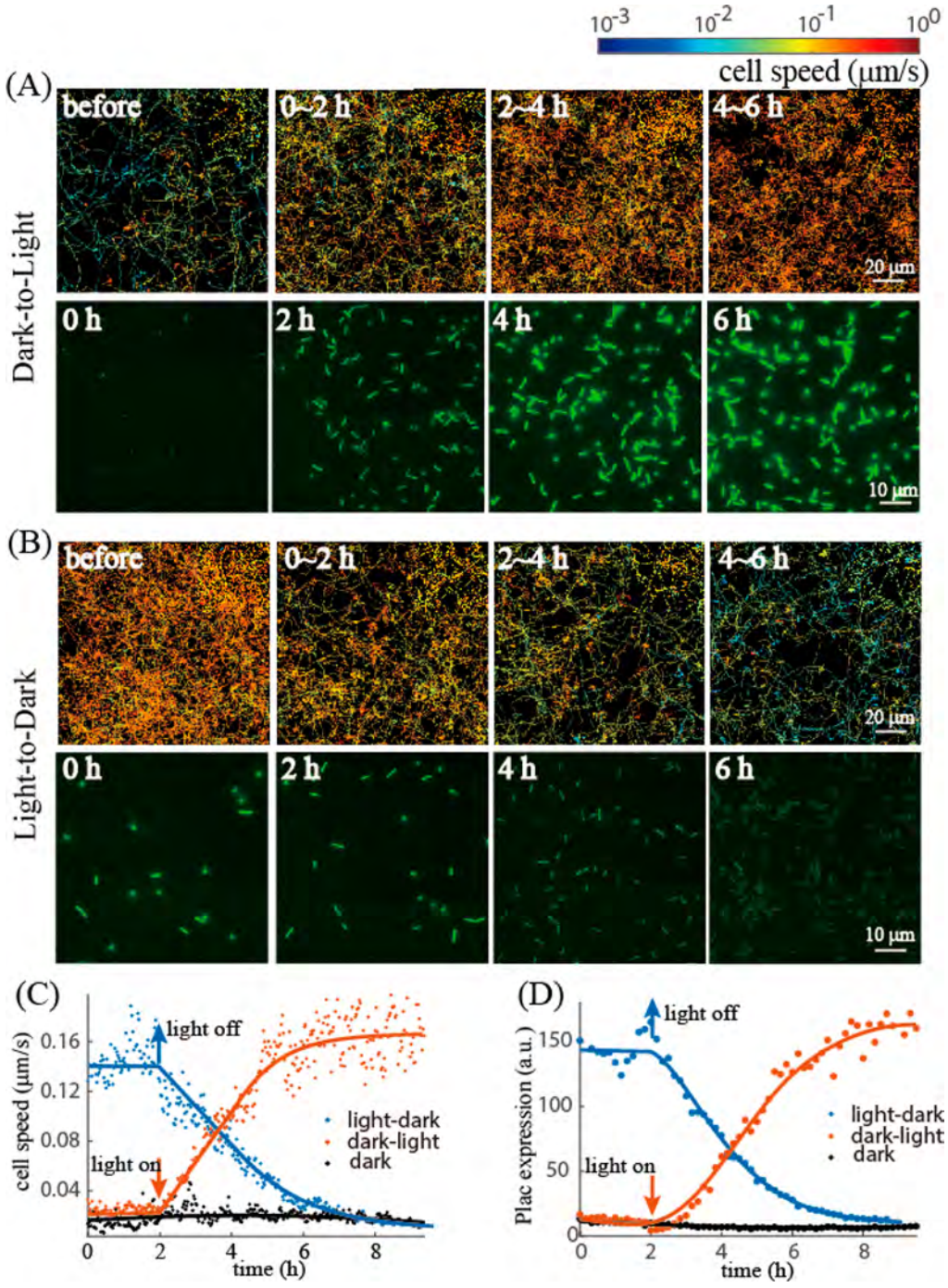

Figure 4. Dynamics and reversibility of twitching manipulation in *pactm*. (A,B) Changes in trajectories or SfGFP expression of *pactm* cells with time during the dark-to-light (A) or the light-to-dark (B) transition. (C,D) Time course of mean cell speed (C) or *Plac* expression (D) of *pactm* cells in response to dark-to-light (red) or light-to-dark (blue) transition or under darkness (dark). The start time of light/dark transition is at 2 h. Recorded experimental data are plotted as dots in the map, and the solid lines represent the smooth results obtained using the Smoothing Spline tool in MATLAB.

the entire population spreads and extends along the illuminated area. To test this speculation, we illuminated a rectangular area connecting two separate colonies (Figure 5C). Due to the limited population, colonies did not exhibit a tendency to spread toward the illumination area during the first 36 h of incubation (Figure 5C). However, both the colonies began to spread toward each other at 36 h, encountered each other at 48 h, and mixed together after 60 h of incubation (Figure 5C). As a control, colonies incubated under darkness for 60 h did not exhibit any tendency to propagate toward each other (Figure 5C). Therefore, we manipulated the twitching direction of bacterial colonies using blue light.

With the development of intestinal microbiology studies, interactions among bacterial species are increasingly attracting attentions.[37−40] Researchers are investigating the interactions of *P. aeruginosa* with *Candida albicans*, *Staphylococcus aureus*, and other species.[41−45] By using our twitching control method,

https://dx.doi.org/10.1021/acssynbio.0c00559
ACS Synth. Biol. 2021, 10, 531−541

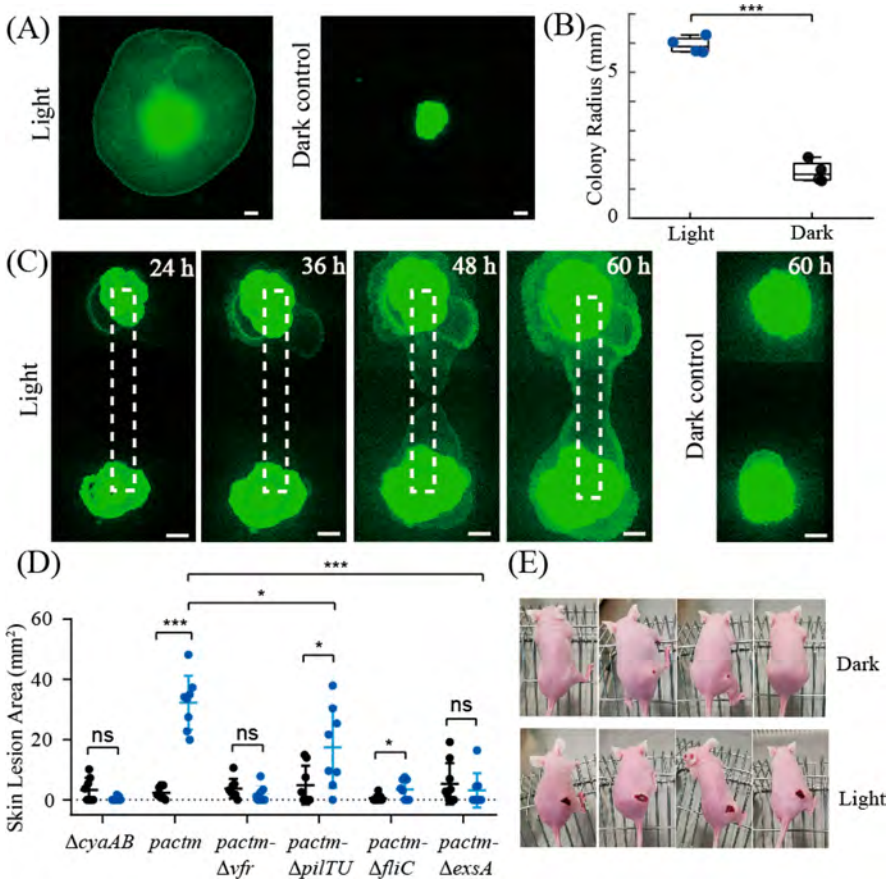

Figure 5. Control of colony propagation and host-infection ability of *pactm* using blue light. (A) SfGFP fluorescent images of 2-day *pactm*Δ*fliC* colonies with (left) or without (right) blue light illumination. Scale bar: 1.0 mm. (B) Radius of 2-day Δ*fliC-pactm* colonies with or without blue light illumination. (C) Time dependent propagation of two separate *pactm*Δ*fliC* colonies connected by a light illuminated rectangular area. The fluorescent image on the far right is the control without blue light illumination at 60 h. Scale bar 1.0 mm. (D) Skin lesion area of BALB-C nude mice infected by Δ*cyaAB*, *pactm*, *pactm*Δ*vfr*, *pactm*Δ*pilTU*, *pactm*Δ*fliC*, or *pactm*Δ*exsA* strain in a 2-day subcutaneous infection model. Mice were kept in darkness (black) or with blue light illumination (blue). (E) Selected photos of *pactm*-infected mice with (down) or without (up) blue light illumination. Statistical analysis based on ANOVA method (ANOVA2 function in MATLAB). *$P < 0.05$; ***$P < 0.001$; ns, nonsignificant.

we could direct two or more bacterial colonies freely toward each other, with a good spatiotemporal resolution. This is extremely useful in the investigation of contact dependent interactions between species, as exemplified by horizontal gene transfer, type VI secretion, and kin selections.

Optical Manipulation of Bacterial Virulence in Mouse Model. To test the effect of light illumination on *pactm* virulence, we injected *pactm* cells subcutaneously in BALBc-nude mice. BALBc-nude mice have no hair to block light and are docile during experimental operations, thus anesthesia could be avoided. Mice were kept in darkness or under blue light illumination, and their skin lesion areas (SLA) were monitored after two-day bacterial inoculation. The *pactm*-infected mice exhibited a 14-fold increase of SLA by blue light (Figure 5D, Figure 5E), whereas the SLAs of both light- and dark-kept mice infected by Δ*cyaA*Δ*cyaB* cells are small and showed no significant difference between each other (Figure 5D). Moreover, mice infected by *pactm*Δ*vfr* cells also exhibited low level and no increase of their SLAs upon light illumination. Therefore, the virulence of *pactm* could be manipulated using blue light and Vfr is the dominant regulator that mediate the upregulated virulence of hyper-cAMP cells. Flagella and type III secretion system were wildly accepted as very important in bacterial acute virulence. As expected, *pactm* strains devoid of flagella or the master regulator of type III secretion system ExsA exhibited significant reduction of their virulence (Figure 5D).

We next examined the role of TFP in the virulence of *pactm*. The role of TFP in host infection has two major aspects: (i) attachment to host cells, which is independent of its motile force and (ii) twitching motility, which is involved in the following step of host invasion.[46] We first knocked out *pilT* and *pilU* in *pactm* and compared its virulence with that of *pactm*. PilT and PilU are the two ATPases involved in TFP retraction in *P. aeruginosa*, *pilT* and *pilU* double mutant cells are completely defective in twitching motility but still protrude their TFP on cell surface that enables bacterial attachment to host cells.[47,48] Under blue light illumination, the SLAs of *pactm*Δ*pilT*Δ*pilU*-infected mice were moderately decreased compare to that of *pactm*-infected mice, suggesting the partial role of twitching motility played during *pactm* infection. Unexpectedly, SLAs of mice infected by *pactm*Δ*pilA* cells, which is devoid of TFP filament, showed 8-fold and 2-fold increase compared to SLAs of *pactm*-infected mice under darkness and blue light, respectively (Figure S4A). The wounds of light-exposed *pactm*Δ*pilA*-infected mice were swelling (Figure S4B), and two of the eight infected mice in the light illumination group were dead after 3-day inoculation. The underlying mechanism of TFP and twitching motility in *pactm* virulence are yet unclear; TFP filaments may also act as

https://dx.doi.org/10.1021/acssynbio.0c00559
ACS Synth. Biol. 2021, 10, 531−541

an antigen that trigger host immune response so that the host can clean out pathogen cells faster.

We also measured several growth curves of *pactm* and related strains under darkness or with blue light illumination (Figure S5). Blue light has slight inhibitory effect on the growth of these strains. According to our results of bacterial virulence in Figure 5D, especially the data of *pactm*Δ*vfr* and Δ*cyaA*Δ*cyaB* control group, the growth inhibitory effect of blue light contributes little to the increased virulence of *pactm*.

DISCUSSIONS

In summary, we have demonstrated that the optogenetic manipulation of intracellular cAMP levels in *P. aeruginosa* could be applied to control its twitching motility and host-infection. Optogenetic control of host-infection has unique advantages over other methods: (i) it does not require chemical inducers that are freely diffusive and may be toxic to the host and (ii) light is easy to obtain and highly tunable, which would simplify experiments. In addition to the host-infection applications, we also successfully directed the propagation of *pactm* colonies by controlling the twitching activity of single cells. This makes *pactm* a candidate tool for application in the investigation of contact-dependent interactions between microbial species. Besides, controlling the collective motion of bacteria may offer an alternative method for bioprinting.

As the start point, duration, and position of light illumination on a host can be controlled precisely, our engineered *pactm* strain provides a flexible and robust tool for the study of host-responses against pathogen invasion. For instance, (i) it could be used to estimate the sensitivity of various tissues to inflammation by illuminating different parts of the host. (ii) By adjusting the intensity and duration of illumination, theoretically, we could continuously regulate the virulence of *pactm* within a certain range, which is particularly useful in quantifying host sensitivity to pathogen invasion. (iii) By turning on light at a particular time, we could precisely control the start point of *pactm* colonization, which may facilitate the study of the dynamic process of initial host response against pathogen invasion. (iv) As the manipulation of intracellular cAMP level in *pactm* is reversible, the subsequent response of host to nonvirulent *P. aeruginosa* could be investigated after infection has been established.

To the best of our knowledge, the present study represents the first demonstration of light-dependent host infection by bacteria. Currently, several improvements are warranted in *pactm*. First, blue light has a relatively low capacity to penetrate tissues, optogenetic tools excited by long wavelength light are generally preferred. During our preparation of this manuscript, a newly developed adenylate cyclase (NIRW-AC) activated by NIRW (near-infrared optical window) light was reported.[4] Although its activation range is narrower than that of bPAC, NIRW-AC is a potential alternative to bPAC. Second, a long time (>3 h) is required for the twitching motility of *pactm* to be fully activated under light illumination or inactivated under darkness, which could limit the utility of *pactm*. Such lengthy activation and inactivation arise from the processes of cAMP accumulation, protein expression, assembly of type III secretion system, or TFP. Since phosphorylation occurs rapidly in bacteria, the development of novel optogenetic tools focusing on protein phosphorylation should reduce the response time of *pactm*.

METHODS

Bacterial strains and plasmids used in the present study are listed in Supplementary Table S1.

Genetic Constructs. The plasmids were constructed using Gibson assembly method. Gene knockouts in *P. aeruginosa* was based on a previous protocol.[49] Refer to Supporting Information for detailed procedures.

Construction of Gene Deletion Mutants in *P. aeruginosa*. PCR was used to generate 1000 bp DNA fragments upstream (Up) or downstream (Dn) from the *pilT, pilU, exsA* and *fliC* genes. The Up and Dn DNA fragments were ligated using overlap extension PCR, and then inserted into pex18gm vector *via* Gibson assembly. The recombinant plasmids were electroporated into *P. aeruginosa*, and the gene knockout mutants were obtained by double selection on LB agar containing 30 μg/mL gentamycin and NaCl-free LB agar containing 15% sucrose at 37 °C.[49] The Up and Dn DNA fragments for *cyaA* and *cyaB* were digested and cloned into pex18ap at *Hin*dIII/XbaI site together with *aacC1*. The recombinant plasmids were electroporated into *P. aeruginosa*, deletion mutants were obtained by selection on LB agar containing 30 μg/mL gentamycin and 5% sucrose at 37 °C. Then the pFLP2 system was used to delete the *aacC1* cassette.[50]

Construction of CTX or Tn7 Plasmids for Chromosomal Gene Expressions in *P. aeruginosa*. To construct the *lacZ*-Tn7 plasmid, PCR fragments of *lacZ* coding sequence and *PA1O4O3* promoter were inserted into the miniTn7 vector *via* Gibson assembly.[51] The resultant plasmid was introduced to target strains through electroporation, and transconjugants were selected on 1.5% LB agar plates supplemented with 30 μg/mL gentamycin. To construct the *pabPAC*-CTX2 plasmid,[31] coding sequence of the original *bPAC* was first optimized for better expression in *P. aeruginosa via* JCat tool (http://www.jcat.de/). The generated *pabPAC* together with a constitutive promoter *J23100* (http://parts.igem.org/Promoters/Catalog/Anderson) was synthesized in GenScript Corporation (Nanjing). PCR fragment of *J23100-pabPAC* was inserted into CTX2 vector *via* Gibson assembly, generating *pabPAC*-CTX2. These resultant plasmid was introduced to target strains through electroporation, and transconjugants were selected on 1.5% LB agar plates supplemented with 100 μg/mL tetracycline (for CTX insertion). The tetracycline resistance cassette in the resultant strain was then deleted according to a standard protocol.[50]

Construction of *Plac* Transcriptional Reporter in *P. aeruginosa*. The *sfGFP* fusion plasmid used to measure the activity of *lac* promoter is a derivative of the vector PUCP20. *lac* promoter sequence together with RNase III sequence, *sfGFP*, *cyOFP1* and terminator fragments were synthesized or amplified using PCR and inserted together into pUCP20 *via* Gibson assembly, generating *Plac*-RNase III-RBS2-*sfGFP*-T_0T_1-J23102-RBS2-*cyOFP1*-T_1-PUCP20, where J23102 is a constitutive promoter (http://parts.igem.org/Promoters/Catalog/Anderson). Constitutively expressed CyOFP1 offers a standard cell identification protocol to avoid failures in cell mask determination when SfGFP intensities are weak. Cell masks identified from CyOFP1 images overlap well with cells in SfGFP images, enabling the quantification of SfGFP fluorescence for *lac* promoter. The reporter plasmid were introduced into *P. aeruginosa* through

https://dx.doi.org/10.1021/acssynbio.0c00559
ACS Synth. Biol. 2021, 10, 531−541

electroporation. Transconjugants were selected on 1.5% LB agar plates supplemented with 30 μg/mL gentamycin.

Cell Growth. Strains were grown on LB agar plates at 37 °C for 20 h from frozen stocks. Monoclonal colonies were inoculated and cultured overnight at 37 °C using a minimal medium (FAB)[52] containing 30 mM sodium glutamate as the carbon source, and harvested at $OD_{600} \sim 2$. Unless otherwise stated, 1 mL of bacterial cultures were cultivated in 5.5 mL polystyrene 12 × 75 mm round-bottom tubes (FALCON #352054) with shaking (250 rpm). Subsequently, the bacterial culture was further diluted (1:100) in the same medium and cultured to $OD_{600} \sim 0.5$ under darkness. 30 μg/mL gentamycin was added to the medium for the culture of strains containing cAMP reporter plasmid. Plates and tubes were wrapped with aluminum foil to achieve dark conditions. The resultant cultures were further diluted 50× in 1 mL of fresh FAB medium before injecting into flow cell. Growth curve experiments in Figure S5 were conducted using LB as culture media at 37 °C, overnight culture (kept in darkness) of each strain in LB were diluted 200 times into fresh LB media, and samples were kept in shaker under blue light illumination (750 $\mu W/cm^2$) or in darkness, three parallel experiments were conducted for each sample.

cAMP Quantification Method. Overnight bacterial culture (kept in darkness at 37 °C) in LB broth were first diluted to $OD_{600} \sim 2.0$ and then diluted 500 times to fresh LB media and grown at 37 °C to $OD_{600} \sim 1.0$ with blue light illumination (750 $\mu W/cm^2$) or under darkness. Bacteria were collected by centrifugation at 12 000g for 3 min at 4 °C and washed twice with 1 mL cold 0.9 M NaCl. Pellets were suspended in 100 μL of 0.1 M HCl and incubated on ice for 20 min with vortexing. Lysates were centrifuged at 12 000g for 10 min at 4 °C to remove cellular material and the supernatant was used for cAMP quantification with an ELISA kit (Sangon Biotech, order # D770001) following the manufacturer's protocol. Duplicate bacterial pellets for protein determination were suspended in 100 μL of PBS buffer and were lysed by four freeze/thaw cycles in liquid nitrogen followed by centrifugation at 12 000g for 10 min, supernatants were collected for BCA protein assay (Sangon Biotech, order # C503021).

Flow Cell Experiments and Imaging. Flow cells (Denmark Technical University) were prepared and sterilized using a standard protocol,[53] and supplemented with FAB medium containing 0.6 mM sodium glutamate and 30 μg/mL gentamycin. All flow cell experiments were conducted at 30 °C, and the flow rate was 3 mL/h. Bacterial cultures (500 μL) were injected into flow cells and the device was left sit for 5 min under darkness to enable initial attachment of cells to the coverslip. Then unattached cells were washed off before cells were observed under a microscope. An inverted fluorescent microscope (IX-71 Olympus) equipped with a 100× oil objective (Olympus) and two sCMOS cameras (Zyla4.2, Andor, 2048 × 2048 pixels) was applied to acquire bright field images (1 frame per second) and fluorescent images (6 frames per hour). Each experiment was performed for more than 7 h, yielding at least 25 000 bright-field images and 84 fluorescent images.

A LED lamp (470L3, THORLABS) was used as the bright-field light source for continuous blue light illumination, and was replaced with a red LED (680L2, THORLABS) when cells were cultured under darkness. Blue light intensity was measured with a power meter (842-PE, Newport). For the characterization of twitching motility under blue light illumination shown in Figure 2(A–E), Figure 3, and Figure 4, light intensity near the bacterial cells was set to 0.7 mW/cm^2. SfGFP, CyOFP1 were excited by light from a 470 nm LED (Lumencor) passing through a bandpass filter (470/20, Semrock). The fluorescence of SfGFP and CyOFP1 were imaged synchronously through one multiband bandpass filter 432/515/595/730 (Semrock), and a emission filter: 520/28 (Semrock) for SfGFP, 583/22 (Semrock) for CyOFP1. The trigger for the on/off state of LEDs, selection of emission filters, and state of cameras for switch between fluorescent and BF image-acquisition were controlled using a microcontroller (Arduino UNO R3).

Image Analysis and Tracking Algorithm. The image analysis software was adapted from methods described previously[32,54] and written in MATLAB (Mathworks). The sfGFP, CyOFP1 and BF images were overlapped using the cp2tform function in the MATLAB function library. The trajectories of the leading pole, trailing pole, and centroid of single cells ($\mathbf{r}_{lead}(t)$, $\mathbf{r}_{trail}(t)$, $\mathbf{r}_{centroid}(t)$) were first denoised using Daubechies wavelet, and the instantaneous velocities ($\mathbf{v}_{lead}(t)$, $\mathbf{v}_{trail}(t)$, $\mathbf{v}_{centroid}(t)$) were calculated subsequently as $\Delta\mathbf{r}(t)/\Delta t$. The time average of the modulus of $\mathbf{v}_{centroid}(t)$ was used to estimate cell speed of single cells. The tilt angle ($\theta(t)$) of cells was estimated using $\theta(t) = \arccos((|\mathbf{r}_{lead}(t) - \mathbf{r}_{trail}(t)| - w)/(l(t) - w))$, where w is the bacterial width, which is nearly independent of time, and $l(t)$ is the bacterial length, which is obtained by linear regression of the time series of projected length ($|\mathbf{r}_{lead}(t) - \mathbf{r}_{trail}(t)|$). The orientation angle of bacterial long axis (φ) was defined as $\varphi = \arccos((x_{lead} - x_{trail})/|\mathbf{r}_{lead} - \mathbf{r}_{trail}|)$, where x_{lead}, x_{trail} are the magnitudes of x-axis, then the instantaneous angular speeds were calculated by $\Delta\varphi(t)/\Delta t$. The mean-square displacement of $\mathbf{r}_{centroid}(t)$ was calculated using $\mathrm{MSD}(\tau) = \frac{1}{T}\int_0^T [\mathbf{r}_{centroid}(t) - \mathbf{r}_{centroid}(t+\tau)]^2 dt$, where T is the duration of trajectory and τ is the time delay. The slope of MSD (k_{MSD}) was obtained from a linear fit of $\log_{10}(\mathrm{MSD})$ as a function of $\log_{10}(\tau)$. To quantify SfGFP intensities from fluorescent images, cell masks were obtained from the CyOFP1 images using a self-written MATLAB code, then the SfGFP fluorescence of cells was measured by counting the mean intensities within corresponding cell masks in the SfGFP images. The image processing code could be download from the group Web site of Jin's group: http://jin.isynbio.siat.ac.cn/wordpress/wp-content/uploads/2019/08/TrackCode.zip.

Twitching Colony Assays. To assay twitching motility on gel–solid surfaces, individual colonies grown on LB agar plates for 20 h at 37 °C were stab inoculated into FAB agarose (1%) with 30 mM sodium glutamate as carbon source. The inoculated agarose was maintained at room temperature under darkness or under the illumination by patterned blue light (0.06 mW/cm^2) from digital-light-processing projector. To illuminate a rectangular area (9 mm × 1 mm) between two colonies, a PowerPoint slide was designed in advance and sent to projector. The PowerPoint slide contained a blue-filled rectangle surrounded by black color, in which blue color represented blue light and black color represented darkness. Fluorescent images of colonies were acquired every 12 h using an inverted microscope (Olympus, IX81) equipped with a 1.25× objective (Olympus, numerical aperture = 0.04).

Subcutaneous Infection Model in Mice. Bacteria of Δ*cyaA*Δ*cyaB*, *pactm*, *pactm*Δ*vfr*, *pactm*Δ*pilT*Δ*pilU*, and

https://dx.doi.org/10.1021/acssynbio.0c00559
ACS Synth. Biol. 2021, 10, 531–541

pactmΔpilA were scrapped from overnight LB agar plates and shook in LB broth containing 30 μg/mL gentamycin for 3 h at 37 °C. The OD_{600} of resultant cultures were diluted to 2.0 and each sample was conducted a further 200 × dilution in fresh LB + 30 μg/mL gentamycin broth and shook for another 3 h at 37 °C. Bacterial culture were harvest at OD_{600} = 0.4−0.5 and washed one time using fresh FAB and diluted to OD_{600} = 0.2 in FAB + 30 mM sodium glutamate. Before injection, all cell suspensions were wrapped in aluminum foil to avoid light exposure.

BALBc-nude female mice were purchased from GemPharmatech Co., Ltd. at 7 weeks of age. All mice were housed in a specific pathogen-free environment at a constant temperature 22 ± 0.3 °C and fed adaptively for 2 days after arrival. Before injection, the injection site of each mouse was washed with 75% ethanol. Bacterial suspensions were injected subcutaneously at the back of the mice slightly near the tail, and each mouse was injected 100 μL of bacterial suspension, resulting in about 2×10^7 initial cells after injection. Usually 16 mice were used for each experiment, with eight mice for the light group and eight mice for the dark group, and four mice were kept in each cage. Mouse cages for dark group experiment were wrapped in aluminum foil, cages for light group were illuminated by blue light (8 mW/cm^2) generated from LED light strip placed right above the cage. In order to dissipate heat, two fans were placed in front of the light group cage to blow wind. SLAs of the infected mice in all group were recorded after 2 days, then the mice were sacrificed. SLA data were processed using GraphPad Prism 8.0. All animals received humane care and experimental protocols were carried out in accordance with the Guide for the Care and Use of Laboratory Animals of University of Science and Technology of China, as approved by the Animal Care Committee of University of Science and Technology of China (USTCACUC192001026).

■ ASSOCIATED CONTENT

Supporting Information

The Supporting Information is available free of charge at https://pubs.acs.org/doi/10.1021/acssynbio.0c00559.

Movie S1 (AVI)

Movie S2 (AVI)

Table S1: Strains and plasmids used in this study; Figure S1: Radius of 2-day Δ*fliC* or *pactm* colonies with or without blue light illumination; Figure S2: Detailed characterization of twitching motility of PAO1 wild type cells with or without blue light illumination; Figure S3: Detailed characterization of twitching motility of *pactmΔvfr* cells with or without blue light illumination; Figure S4: Skin lesion area of BALB-C nude mice infected by *pactm* and *pactmΔpilA* strain in a 2-day subcutaneous infection model; Figure S5: Growth curves of pactm, ΔcyaAΔcyaB, PAO1, and *pactmΔvfr* strains under blue light illumination or darkness (PDF)

■ AUTHOR INFORMATION

Corresponding Authors

Zhi Liu − *Department of Biotechnology, College of Life Science and Technology, Huazhong University of Science and Technology, Wuhan 430074, PR China*; Email: zhiliu@hust.edu.cn

Lei Ni − *CAS Key Laboratory of Quantitative Engineering Biology, Shenzhen Institute of Synthetic Biology, Shenzhen Institutes of Advanced Technology, Chinese Academy of Sciences, Shenzhen 518055, PR China*; Email: lei.ni@siat.ac.cn

Fan Jin − *CAS Key Laboratory of Quantitative Engineering Biology, Shenzhen Institute of Synthetic Biology, Shenzhen Institutes of Advanced Technology, Chinese Academy of Sciences, Shenzhen 518055, PR China; Hefei National Laboratory for Physical Sciences at the Microscale, University of Science and Technology of China, Hefei, Anhui 230026, PR China*; orcid.org/0000-0003-2313-0388; Email: fan.jin@siat.ac.cn

Authors

Aiguo Xia − *CAS Key Laboratory of Quantitative Engineering Biology, Shenzhen Institute of Synthetic Biology, Shenzhen Institutes of Advanced Technology, Chinese Academy of Sciences, Shenzhen 518055, PR China*

Mingjie Qian − *Department of Biotechnology, College of Life Science and Technology, Huazhong University of Science and Technology, Wuhan 430074, PR China*

Congcong Wang − *Department of Chemical Physics, University of Science and Technology of China, Hefei, Anhui 230026, PR China*

Yajia Huang − *CAS Key Laboratory of Quantitative Engineering Biology, Shenzhen Institute of Synthetic Biology, Shenzhen Institutes of Advanced Technology, Chinese Academy of Sciences, Shenzhen 518055, PR China*

Complete contact information is available at: https://pubs.acs.org/10.1021/acssynbio.0c00559

Author Contributions

Conceptualization: Fan Jin, Zhi Liu. Methodology: Mingjie Qian, Aiguo Xia, Congcong Wang, Yajia Huang, Lei Ni. Investigation: Aiguo Xia, Lei Ni, Fan Jin. Writing (original draft): Lei Ni, Aiguo Xia. Writing (review and editing): Fan Jin.

Notes

The authors declare no competing financial interest.

■ ACKNOWLEDGMENTS

We thank J.D. Shrout for providing the PAO1 strain. This work was supported by the National Key Research and Development Program of China (2020YFA0906900 and 2018YFA0902700) and the National Natural Science Foundation of China (31700087, 21774117, 31700745, 31770132, 81572050) and the Fundamental Research Funds for the Central Universities (WK3450000003) supported this work.

■ REFERENCES

(1) Abell, C. W., and Monahan, T. M. (1973) Role of Adenosine 3′,5′-Cyclic Monophosphate in Regulation of Mammalian-Cell Division. *J. Cell Biol. 59*, 549−558.

(2) Conti, M. (2002) Specificity of the cyclic adenosine 3 ‘,5 ‘-monophosphate signal in granulosa cell function. *Biol. Reprod. 67*, 1653−1661.

(3) Richards, J. S. (2001) New signaling pathways for hormones and cyclic adenosine 3 ‘,5 ‘-monophosphate action in endocrine cells. *Mol. Endocrinol. 15*, 209−218.

(4) Fomicheva, A., Zhou, C., Sun, Q.-Q., and Gomelsky, M. (2019) Engineering Adenylate Cyclase Activated by Near-Infrared Window Light for Mammalian Optogenetic Applications. *ACS Synth. Biol. 8*, 1314−1324.

(5) Iseki, M., Matsunaga, S., Murakami, A., Ohno, K., Shiga, K., Yoshida, K., Sugai, M., Takahashi, T., Hori, T., and Watanabe, M. (2002) A blue-light-activated adenylyl cyclase mediates photoavoidance in *Euglena gracilis*. *Nature 415*, 1047−1051.
(6) Scheib, U., Broser, M., Constantin, O. M., Yang, S., Gao, S., Mukherjee, S., Stehfest, K., Nagel, G., Gee, C. E., and Hegemann, P. (2018) Rhodopsin-cyclases for photocontrol of cGMP/cAMP and 2.3 Å structure of the adenylyl cyclase domain. *Nat. Commun. 9*, 2046.
(7) Stierl, M., Stumpf, P., Udwari, D., Gueta, R., Hagedorn, R., Losi, A., Gärtner, W., Petereit, L., Efetova, M., Schwarzel, M., Oertner, T. G., Nagel, G., and Hegemann, P. (2011) Light modulation of cellular cAMP by a small bacterial photoactivated adenylyl cyclase, bPAC, of the soil bacterium *Beggiatoa*. *J. Biol. Chem. 286*, 1181−1188.
(8) Ryu, M.-H., Kang, I.-H., Nelson, M. D., Jensen, T. M., Lyuksyutova, A. I., Siltberg-Liberles, J., Raizen, D. M., and Gomelsky, M. (2014) Engineering adenylate cyclases regulated by near-infrared window light. *Proc. Natl. Acad. Sci. U. S. A. 111*, 10167−10172.
(9) De Marco, R. J., Thiemann, T., Groneberg, A. H., Herget, U., and Ryu, S. (2016) Optogenetically enhanced pituitary corticotroph cell activity post-stress onset causes rapid organizing effects on behaviour. *Nat. Commun.*, 12620.
(10) Hartmann, A., Arroyo-Olarte, R. D., Imkeller, K., Hegemann, P., Lucius, R., and Gupta, N. (2013) Optogenetic Modulation of an Adenylate Cyclase in Toxoplasma gondii Demonstrates a Requirement of the Parasite cAMP for Host-Cell Invasion and Stage Differentiation. *J. Biol. Chem. 288*, 13705−13717.
(11) Jansen, V., Alvarez, L., Balbach, M., Struenker, T., Hegemann, P., Kaupp, U. B., and Wachten, D. (2015) Controlling fertilization and cAMP signaling in sperm by optogenetics. *eLife*, DOI: 10.7554/eLife.05161.
(12) Louis, T., Stahl, A., Boto, T., and Tomchik, S. M. (2018) Cyclic AMP-dependent plasticity underlies rapid changes in odor coding associated with reward learning. *Proc. Natl. Acad. Sci. U. S. A. 115*, E448−E457.
(13) Sample, V., DiPilato, L. M., Yang, J. H., Ni, Q., Saucerman, J. J., and Zhang, J. (2012) Regulation of nuclear PKA revealed by spatiotemporal manipulation of cyclic AMP. *Nat. Chem. Biol. 8*, 375−382.
(14) O'Banion, C. P., Vickerman, B. M., Haar, L., and Lawrence, D. S. (2019) Compartmentalized cAMP Generation by Engineered Photoactivated Adenylyl Cyclases. *Cell Chem. Biol. 26*, 1393−1406.
(15) Beatson, S. A., Whitchurch, C. B., Sargent, J. L., Levesque, R. C., and Mattick, J. S. (2002) Differential regulation of twitching motility and elastase production by Vfr in *Pseudomonas aeruginosa*. *J. Bacteriol. 184*, 3605−3613.
(16) Ferenci, T. (1996) Adaptation to life at micromolar nutrient levels: The regulation of *Escherichia coli* glucose transport by endoinduction and cAMP. *FEMS Microbiol. Rev. 18*, 301−317.
(17) Green, J., Stapleton, M. R., Smith, L. J., Artymiuk, P. J., Kahramanoglou, C., Hunt, D. M., and Buxton, R. S. (2014) Cyclic-AMP and bacterial cyclic-AMP receptor proteins revisited: adaptation for different ecological niches. *Curr. Opin. Microbiol. 18*, 1−7.
(18) Kalia, D., Merey, G., Nakayama, S., Zheng, Y., Zhou, J., Luo, Y., Guo, M., Roembke, B. T., and Sintim, H. O. (2013) Nucleotide, c-di-GMP, c-di-AMP, cGMP, cAMP, (p)ppGpp signaling in bacteria and implications in pathogenesis. *Chem. Soc. Rev. 42*, 305−341.
(19) Liang, W., Pascual-Montano, A., Silva, A. J., and Benitez, J. A. (2007) The cyclic AMP receptor protein modulates quorum sensing, motility and multiple genes that affect intestinal colonization in Vibrio cholerae. *Microbiology 153*, 2964−2975.
(20) Poncet, S., Milohanic, E., Maze, A., Abdallah, J. N., Ake, F., Larribe, M., Deghmane, A.-E., Taha, M.-K., Dozot, M., De Bolle, X., Letesson, J. J., and Deutscher, J. (2009) Correlations between carbon metabolism and virulence in bacteria. *Contrib. Microbiol. 16*, 88−102.
(21) Fuchs, E. L., Brutinel, E. D., Jones, A. K., Fulcher, N. B., Urbanowski, M. L., Yahr, T. L., and Wolfgang, M. C. (2010) The *Pseudomonas aeruginosa* Vfr Regulator Controls Global Virulence Factor Expression through Cyclic AMP-Dependent and -Independent Mechanisms. *J. Bacteriol. 192*, 3553−3564.
(22) Fulcher, N. B., Holliday, P. M., Klem, E., Cann, M. J., and Wolfgang, M. C. (2010) The *Pseudomonas aeruginosa* Chp chemosensory system regulates intracellular cAMP levels by modulating adenylate cyclase activity. *Mol. Microbiol. 76*, 889−904.
(23) Jansari, V. H., Potharla, V. Y., Riddell, G. T., and Bardy, S. L. (2016) Twitching motility and cAMP levels: signal transduction through a single methyl-accepting chemotaxis protein. *FEMS Microbiol. Lett.*, DOI: 10.1093/femsle/fnw119.
(24) Marsden, A. E., Intile, P. J., Schulmeyer, K. H., Simmons-Patterson, E. R., Urbanowski, M. L., Wolfgang, M. C., and Yahr, T. L. (2016) Vfr Directly Activates *exsA* Transcription To Regulate Expression of the *Pseudomonas aeruginosa* Type III Secretion System. *J. Bacteriol. 198*, 1442−1450.
(25) Whitchurch, C. B., Beatson, S. A., Comolli, J. C., Jakobsen, T., Sargent, J. L., Bertrand, J. J., West, J., Klausen, M., Waite, L. L., Kang, P. J., Tolker-Nielsen, T., Mattick, J. S., and Engel, J. N. (2005) *Pseudomonas aeruginosa fimL* regulates multiple virulence functions by intersecting with Vfr-modulated pathways. *Mol. Microbiol. 55*, 1357−1378.
(26) Wolfgang, M. C., Lee, V. T., Gilmore, M. E., and Lory, S. (2003) Coordinate regulation of bacterial virulence genes by a novel adenylate cyclase-dependent signaling pathway. *Dev. Cell 4*, 253−263.
(27) Heiniger, R. W., Winther-Larsen, H. C., Pickles, R. J., Koomey, M., and Wolfgang, M. C. (2010) Infection of human mucosal tissue by *Pseudomonas aeruginosa* requires sequential and mutually dependent virulence factors and a novel pilus-associated adhesin. *Cell. Microbiol. 12*, 1158−1173.
(28) Davinic, M., Carty, N. L., Colmer-Hamood, J. A., Francisco, M. S., and Hamood, A. N. (2009) Role of Vfr in regulating exotoxin A production by *Pseudomonas aeruginosa*. *Microbiology 155*, 2265−2273.
(29) Ferrell, E., Carty, N. L., Colmer-Hamood, J. A., Hamood, A. N., and West, S. E. H. (2008) Regulation of *Pseudomonas aeruginosa* ptxR by Vfr. *Microbiology 154*, 431−439.
(30) Kanack, K. J., Runyen-Janecky, L. J., Ferrell, E. P., Suh, S.-J., and West, S. E. H. (2006) Characterization of DNA-binding specificity and analysis of binding sites of the *Pseudomonas aeruginosa* global regulator, Vfr, a homologue of the *Escherichia coli* cAMP receptor protein. *Microbiology 152*, 3485−3496.
(31) Hoang, T. T., Kutchma, A. J., Becher, A., and Schweizer, H. P. (2000) Integration-proficient plasmids for *Pseudomonas aeruginosa*: Site-specific integration and use for engineering of reporter and expression strains. *Plasmid 43*, 59−72.
(32) Ni, L., Yang, S., Zhang, R., Jin, Z., Chen, H., Conrad, J. C., and Jin, F. (2016) Bacteria differently deploy type-IV pili on surfaces to adapt to nutrient availability. *npj Biofilms Microbiomes*, DOI: 10.1038/npjbiofilms.2015.29.
(33) Skerker, J. M., and Berg, H. C. (2001) Direct observation of extension and retraction of type IV pili. *Proc. Natl. Acad. Sci. U. S. A. 98*, 6901−6904.
(34) Gibiansky, M. L., Conrad, J. C., Jin, F., Gordon, V. D., Motto, D. A., Mathewson, M. A., Stopka, W. G., Zelasko, D. C., Shrout, J. D., and Wong, G. C. L. (2010) Bacteria Use Type IV Pili to Walk Upright and Detach from Surfaces. *Science 330*, 197−197.
(35) Clausen, M., Koomey, M., and Maier, B. (2009) Dynamics of Type IV Pili Is Controlled by Switching Between Multiple States. *Biophys. J. 96*, 1169−1177.
(36) Rashid, M. H., and Kornberg, A. (2000) Inorganic polyphosphate is needed for swimming, swarming, and twitching motilities of *Pseudomonas aeruginosa*. *Proc. Natl. Acad. Sci. U. S. A. 97*, 4885−4890.
(37) Fons, A. G. T. K. M. (2000) Mechanisms of Colonisation and Colonisation Resistance of the Digestive Tract Part 2: Bacteria/Bacteria Interactions. *Microb. Ecol. Health Dis. 12*, 240−246.
(38) Dillon, R. J., and Dillon, V. M. (2004) The gut bacteria of insects: Nonpathogenic interactions. *Annu. Rev. Entomol. 49*, 71−92.
(39) Federle, M. J., and Bassler, B. L. (2003) Interspecies communication in bacteria. *J. Clin. Invest. 112*, 1291−1299.
(40) Fraune, S., Anton-Erxleben, F., Augustin, R., Franzenburg, S., Knop, M., Schroeder, K., Willoweit-Ohl, D., and Bosch, T. C. G.

(2015) Bacteria-bacteria interactions within the microbiota of the ancestral metazoan Hydra contribute to fungal resistance. *ISME J. 9*, 1543−1556.
(41) Alves, P. M., Al-Badi, E., Withycombe, C., Jones, P. M., Purdy, K. J., and Maddocks, S. E. (2018) Interaction between *Staphylococcus aureus* and *Pseudomonas aeruginosa* is beneficial for colonisation and pathogenicity in a mixed biofilm. *Pathog. Dis.*, DOI: 10.1093/femspd/fty003.
(42) Armbruster, C. R., Wolter, D. J., Mishra, M., Hayden, H. S., Radey, M. C., Merrihew, G., MacCoss, M. J., Burns, J., Wozniak, D. J., Parsek, M. R., and Hoffman, L. R. (2016) *Staphylococcus aureus* Protein A Mediates Interspecies Interactions at the Cell Surface of *Pseudomonas aeruginosa*. *mBio*, DOI: 10.1128/mBio.00538-16.
(43) Beaudoin, T., Yau, Y. C. W., Stapleton, P. J., Gong, Y., Wang, P. W., Guttman, D. S., and Waters, V. (2017) *Staphylococcus aureus* interaction with *Pseudomonas aeruginosa* biofilm enhances tobramycin resistance. *npj Biofilms Microbiomes*, DOI: 10.1038/s41522-017-0035-0.
(44) DeLeon, S., Clinton, A., Fowler, H., Everett, J., Horswill, A. R., and Rumbaugh, K. P. (2014) Synergistic Interactions of *Pseudomonas aeruginosa* and *Staphylococcus aureus* in an In Vitro Wound Model. *Infect. Immun. 82*, 4718−4728.
(45) Fourie, R., Ells, R., Swart, C. W., Sebolai, O. M., Albertyn, J., and Pohl, C. H. (2016) Candida albicans and *Pseudomonas aeruginosa* Interaction, with Focus on the Role of Eicosanoids. *Front. Physiol.*, DOI: 10.3389/fphys.2016.00064.
(46) Burrows, L. L. (2012) *Pseudomonas aeruginosa* Twitching Motility: Type IV Pili in Action, In *Annu. Rev. Microbiol.* (Gottesman, S., Harwood, C. S., and Schneewind, O., Eds.) Vol *66*, pp 493−520.
(47) Whitchurch, C. B., and Mattick, J. S. (1994) Characterization of a gene, pilU, required for twitching motility but not phage sensitivity in *Pseudomonas aeruginosa*. *Mol. Microbiol. 13*, 1079−1091.
(48) Comolli, J. C., Hauser, A. R., Waite, L., Whitchurch, C. B., Mattick, J. S., and Engel, J. N. (1999) *Pseudomonas aeruginosa* gene products PilT and PilU are required for cytotoxicity in vitro and virulence in a mouse model of acute pneumonia. *Infect. Immun. 67*, 3625−3630.
(49) Hmelo, L. R., Borlee, B. R., Almblad, H., Love, M. E., Randall, T. E., Tseng, B. S., Lin, C., Irie, Y., Storek, K. M., Yang, J. J., Siehnel, R. J., Howell, P. L., Singh, P. K., Tolker-Nielsen, T., Parsek, M. R., Schweizer, H. P., and Harrison, J. J. (2015) Precision-engineering the *Pseudomonas aeruginosa* genome with two-step allelic exchange. *Nat. Protoc. 10*, 1820.
(50) Hoang, T. T., Karkhoff-Schweizer, R. R., Kutchma, A. J., and Schweizer, H. P. (1998) A broad-host-range Flp-FRT recombination system for site-specific excision of chromosomally-located DNA sequences: application for isolation of unmarked *Pseudomonas aeruginosa* mutants. *Gene 212*, 77−86.
(51) Choi, K. H., and Schweizer, H. P. (2006) mini-Tn7 insertion in bacteria with single attTn7 sites: example *Pseudomonas aeruginosa*. *Nat. Protoc. 1*, 153−161.
(52) Pu, L., Yang, S., Xia, A., and Jin, F. (2018) Optogenetics Manipulation Enables Prevention of Biofilm Formation of Engineered *Pseudomonas aeruginosa* on Surfaces. *ACS Synth. Biol. 7*, 200−208.
(53) Heydorn, A., Ersbøll, B. K., Hentzer, M., Parsek, M. R., Givskov, M., and Molin, S. (2000) Experimental reproducibility in flow-chamber biofilms. *Microbiology 146*, 2409−2415.
(54) Jin, F., Conrad, J. C., Gibiansky, M. L., and Wong, G. C. L. (2011) Bacteria use type-IV pili to slingshot on surfaces. *Proc. Natl. Acad. Sci. U. S. A. 108*, 12617−12622.

https://dx.doi.org/10.1021/acssynbio.0c00559
ACS Synth. Biol. 2021, 10, 531−541